



NIH PUBLIC ACCESS

Author Manuscript

Osteoarthritis Cartilage. Author manuscript; available in PMC 2012 January 12.

Published in final edited form as:

Osteoarthritis Cartilage. 2010 December ; 18(12): 1608–1619. doi:10.1016/j.joca.2010.09.004.

Effect of Self-assembling Peptide, Chondrogenic Factors, and Bone Marrow Derived Stromal Cells on Osteochondral Repair

Rachel E. Miller, Ph.D.¹, Alan J. Grodzinsky, Sc.D.^{1,2}, Eric J. Vanderploeg, Ph.D.², Christina Lee, Ph.D.³, Dora J. Ferris, DVM³, Myra F. Barrett, DVM^{3,4}, John D. Kisiday, Ph.D.³, and David D. Frisbie, DVM, Ph.D.³[Diplomate ACVS]

¹ Department of Biological Engineering, Massachusetts Institute of Technology, Cambridge, MA

² Center for Biomedical Engineering, Massachusetts Institute of Technology, Cambridge, MA

³ Colorado State University, Equine Orthopaedic Research Center, Fort Collins, CO

⁴ Colorado State University, Department of Environmental Health and Radiological Sciences, Fort Collins, CO

Abstract

Objective—The goal of this study was to test the ability of an injectable self-assembling peptide (KLD) hydrogel with or without chondrogenic factors (CF) and allogeneic bone marrow stromal cells (BMSCs) to stimulate cartilage regeneration in a full-thickness, critically-sized, rabbit cartilage defect model *in vivo*. We used CF treatments to test the hypotheses that CF would stimulate chondrogenesis and matrix production by cells migrating into acellular KLD (KLD+CF) or by BMSCs delivered in KLD (KLD+CF+BMSCs).

Design—Three groups were tested against contralateral untreated controls: KLD, KLD+CF, and KLD+CF+BMSCs, n=6–7. TGF- β 1, dexamethasone, and IGF-1 were used as chondrogenic factors (CF) pre-mixed with KLD and BMSCs before injection. Evaluations included gross, histological, immunohistochemical and radiographic analyses.

Results—KLD without CF or BMSCs showed the greatest repair after 12 weeks with significantly higher Safranin-O, collagen II immunostaining, and cumulative histology scores than untreated contralateral controls. KLD+CF resulted in significantly higher aggrecan immunostaining than untreated contralateral controls. Including allogeneic BMSCs+CF markedly reduced the quality of repair and increased osteophyte formation compared to KLD alone.

Corresponding author: David D Frisbie; CSU Orthopaedic Research Center, College of Veterinary Medicine and Biomedical Sciences, 300 West Drake Road, Fort Collins, Colorado 80523, Phone: (970) 297-4555, Fax: (970) 297-4138, dfrisbie@colostate.edu.

CONFLICT OF INTEREST: No conflicts of interest to report.

AUTHOR CONTRIBUTIONS: Rachel E. Miller: conception, analysis and interpretation, drafting

Alan J. Grodzinsky: conception, interpretation, revising, funding (alg@mit.edu)

Eric J. Vanderploeg: conception, revising

Christina Lee: acquisition of data, revising

Dora J. Ferris: acquisition of data, revising

Myra F. Barrett: acquisition of data, revising

John D. Kisiday: conception, acquisition, revising

David D. Frisbie: conception, acquisition, analysis, statistical expertise, interpretation, revising, funding (dfrisbie@colostate.edu)

Publisher's Disclaimer: This is a PDF file of an unedited manuscript that has been accepted for publication. As a service to our customers we are providing this early version of the manuscript. The manuscript will undergo copyediting, typesetting, and review of the resulting proof before it is published in its final citable form. Please note that during the production process errors may be discovered which could affect the content, and all legal disclaimers that apply to the journal pertain.

Conclusions—These data show that KLD can fill full-thickness osteochondral defects in situ and improve cartilage repair as shown by Safranin-O, collagen II immunostaining, and cumulative histology. In this small animal model, the full-thickness critically-sized defect provided access to the marrow, similar in concept to abrasion arthroplasty or spongyalization in large animal models, and suggests that combining KLD with these techniques may improve current practice.

Keywords

Bone marrow derived mesenchymal stem cells; cartilage; tissue engineering; rabbit model; self-assembling peptide scaffold

INTRODUCTION

Repair of articular cartilage injuries remains a challenge, despite the development of surgical treatments such as microfracture, abrasion arthroplasty, and spongyalization, which are used with the goal of recruiting marrow-derived cells by penetration of the subchondral bone. While these techniques promote increased short-term healing, long-term repair still consists of mechanically-inferior fibrocartilage¹. Recent research has focused on tissue engineering strategies using scaffolds to improve cartilage repair and regeneration. In particular, hydrogels made from materials such as chitosan-glycerol phosphate², polyethyleneglycol (PEG)³, fibrin⁴, polyglycolic-co-lactic acid (PLGA)⁵, and collagen⁶ have been explored with the goal of improving the accumulation of extracellular matrix produced by cells (e.g., bone marrow stromal cells (BMSCs)) migrating into the scaffold from marrow.

Stimulation of BMSC chondrogenesis *in vitro* and *in vivo* has received much attention. *In vitro* studies have shown that transforming growth factor- β 1 (TGF- β 1), dexamethasone, and insulin-like growth factor-1 (IGF-1) promote chondrogenesis of BMSCs^{7–11}, and methods for delivering these chondrogenic factors have been developed, often in conjunction with scaffolds^{12–15}. There have been a number of *in vivo* studies performed delivering IGF-1^{4,16}, TGF- β 1^{1,17,18}, or the combination of IGF-1 and TGF- β 1^{13,16,19} to cartilage defects in order to stimulate chondrogenesis of endogenous BMSCs, but to our knowledge, no *in vivo* studies have incorporated dexamethasone.

The hypothesis that delivery of exogenous BMSCs to the joint can enhance cartilage regeneration has prompted the exploration of a wide variety of growth factor and scaffold combinations to stimulate BMSC chondrogenesis^{1,20,21}. *In vivo* studies have attempted to deliver BMSCs alone^{22,23}, BMSCs encapsulated in scaffolds^{24–26}, and BMSCs encapsulated in scaffolds with the inclusion of TGF- β 1^{27–30}. Despite the *in vitro* promise shown by 3D-cultured BMSCs, most long-term *in vivo* treatments with BMSCs have resulted in sub-optimal cartilage repair tissue^{20,22,24,26}. Improving BMSC chondrogenesis *in vivo* is likely dependent on several factors that are not well understood, including cell delivery, microenvironment, and a combination of pro-chondrogenic longitudinal signaling. In addition, an ideal clinical approach would minimize or obviate the *in vitro* culture duration and be performed with a single arthroscopic procedure.

Recent studies have shown that hydrogels made from the self-assembling peptide sequences (RADA)₄ and (KLDL)₃ (hereafter referred to as KLD) can maintain the chondrocyte phenotype³¹ and stimulate chondrogenesis of BMSCs *in vitro*^{32–34}. These hydrogels have the ability to rapidly assemble when exposed to physiological pH and ionic strength³⁵ and have pore sizes in the range of 100–500 nm³⁶. These synthetic peptides have been used *in vivo* without immunogenic reaction³⁷. Furthermore, TGF- β 1 has been shown to adsorb to KLD when pre-mixed with the peptide solution prior to assembly, resulting in extended delivery of TGF- β 1 to BMSCs and stimulating chondrogenesis *in vitro*, promoting sGAG

production and accumulation comparable to continuous medium supplementation of TGF- β 1 over 21 days³⁸. In addition, including dexamethasone with TGF- β 1 in medium supplementation during the *in vitro* culture of BMSCs in RADA results in less catabolic cleavage of aggrecan compared to culture with TGF- β 1 alone³⁹. Finally, IGF-1 can be tethered to peptide scaffolds via biotin-streptavidin bonds; this tethered IGF-1 has been shown to remain biologically active and to promote cell survival in rat cardiomyocytes over 28 days³⁷.

The goal of this study was to test the ability of an injectable KLD hydrogel with or without BMSCs and chondrogenic factors (CF) to stimulate cartilage regeneration *in vivo* in a critically-sized rabbit full-thickness cartilage defect model. This model provides access to the marrow, analogous to abrasion arthroplasty or spongiolization in large animal models. We used CF treatments (IGF-1, TGF- β 1, and dexamethasone) to test the hypotheses that CF would stimulate chondrogenesis and matrix production (1) by cells migrating into acellular KLD and (2) by P2 passaged allogeneic BMSCs delivered in KLD. IGF-1 was tethered to the peptide with a biotin-streptavidin bond³⁷ to stimulate long-term production of cartilage ECM, while TGF- β 1 and dexamethasone were pre-mixed with KLD prior to BMSC encapsulation to stimulate chondrogenesis and initial matrix production. A 12-week timepoint enabled evaluation of mid-term benefits of the treatment compared to contralateral untreated defects.

METHODS

Materials

KLD peptide with the sequence AcN-(KLDL)₃-CNH₂ was synthesized by the MIT Biopolymers Laboratory (Cambridge, MA) using an ABI Model 433A peptide synthesizer with Fmoc protection. Human recombinant TGF- β 1 (R&D Systems, Inc., Minneapolis, MN), dexamethasone (Sigma-Aldrich, St. Louis, MO), sucrose (Sigma-Aldrich), biotinylated-IGF-1 (bIGF-1) (immunological and biochemical test systems GmbH, Reutlingen Germany), streptavidin (Pierce Biotechnology, Inc, Rockford, IL), biotinylated-KLD (biotin-(aminocaproic acid)₃-(KLDL)₃ or b-KLD) (MIT Biopolymers Laboratory), FBS (Invitrogen, Carlsbad, CA), and FGF-2 (R&D Systems, Inc.) were purchased and used as described.

Cell Isolation

Bone marrow was harvested and pooled from four rabbits used for an initial pilot study, and BMSCs were isolated as previously described³⁴. BMSCs were selected via differential adhesion to plastic and expanded two passages in alphaMEM with 10% FBS and 2 ng/mL FGF-2, 10 mM HEPES, and PSA (100 U/mL penicillin, 100 μ g/mL streptomycin, and 250 ng/mL amphotericin), resulting in a total of approximately four population doublings. Each passage was conducted by seeding at a concentration of 12×10^3 BMSCs/cm² and incubating for two days to allow BMSCs to grow to ~75% confluence.

In Vivo Study Design

All procedures were approved by the Animal Care and Use Committees at Colorado State University and Massachusetts Institute of Technology. Twenty skeletally mature, retired, female breeder New Zealand White rabbits (average age 11 months and body weight 4.7 kg) were used for this study (Myrtle's Rabbitry, Thompson Station, TN). One rabbit died during the study due to neurologic problems post-surgery and was not included in the analysis. The n values shown in Table 1 do not reflect this animal. Three different groups were tested against contralateral, untreated, empty controls: (1) KLD, (2) KLD+chondrogenic factors (CF), and (3) KLD+CF+BMSCs (Table 1). For all groups, KLD was resuspended in 10%

sterile sucrose, and the final KLD concentration was kept constant at 3.2 mg/mL. For groups 2 and 3, KLD peptide (48 μ g) was pre-mixed with a CF mixture consisting of 1.4 ng TGF- β 1, 0.6 ng dexamethasone, 4.1 ng biotinylated-IGF-1 (bIGF-1), 30.7 ng streptavidin, and 0.48 μ g b-KLD. For group 3, 150×10^3 BMSCs were encapsulated in the KLD/CF mixture³⁴. Encapsulation of BMSCs *in vitro* in this manner resulted in 80–90% viability. *In vitro* studies indicated that this amount of TGF- β 1 would result in a concentration of TGF- β 1 inside the scaffold sufficient to stimulate chondrogenesis³⁸. At the same time, if all of the TGF- β 1 were to be released from the scaffold at once into the joint space *in vivo*, it would amount to approximately 1 ng/mL concentration in the joint space (1.4 ng/1.4 mL joint space volume⁴⁰), compared to the native concentration of 52.3 pg/mL found in adult rabbits⁴⁰. Streptavidin and bIGF-1 were mixed at a 1:1 molar ratio in order to achieve, on average, binding of one bIGF-1 to each streptavidin allowing streptavidin to still bind b-KLD (in 100x molar excess of streptavidin and bIGF-1 to ensure homogeneous distribution of IGF-1 throughout the gel). The ability of this tethering to occur using these molar ratios has been shown *in vitro* and *in vivo*³⁷. The amount of bIGF-1 tethered was chosen to provide a local concentration of 300 ng/mL inside the scaffold, which is above the threshold shown to be sufficient for chondrocyte stimulation of proteoglycan synthesis *in vivo*⁴¹.

Defect Creation and Gel Injection

All surgical procedures were performed under inhalation general anesthesia. A medial-parapatellar arthrotomy approach to the femoropatellar joint was performed, and the patella was luxated laterally. A 3mm-diam \times 2mm-deep full-thickness, critically-sized defect was created in the central region of the femoral trochlear groove (Fig 1). Direct pressure was applied with a surgical sponge to ensure all bleeding was stopped prior to application of the peptide, which was delivered as a liquid. Defects were filled with designated treatments (15 μ L volume) or left untreated, as dictated by group assignment. The liquid peptide suspension could easily be seen filling the defect, and defects were filled until visually full. At this time, Lactated Ringer's Solution was added to the joint periphery to gently fill the joint and cause polymerization of the peptide, which was visually inspected to ensure retention of the implant. Dorsal-caudal and lateral-medial 90° radiographs of each stifle joint were obtained immediately after surgery. At 12 weeks, rabbits were euthanized with pentobarbital after sedation. Post-surgical radiographic views were repeated following euthanasia.

Gross Pathologic Observations of Joints

The limbs and joints were examined and graded by a blinded observer (DDF) unaware of treatment group (Table 2). For the muscle wastage measurement, the limbs were shaved and a flexible tape measure was used in a similar anatomic location of the stifle to make this assessment. This scoring system was chosen in order to compare to other studies performed by Frisbie et al.⁶

Synovial Membrane Histology

Synovial membrane was harvested and placed in neutral-buffered 10% formalin, embedded in paraffin, 5- μ m sections created and stained with hematoxylin and eosin (H&E). Sections were evaluated blindly (DDF) for cellular infiltration, vascularity, intimal hyperplasia, subintimal edema and subintimal fibrosis on a scale of 0–4 (0=none, 1=slight, 2=mild, 3=moderate, 4=severe)⁴².

Articular Cartilage Histology and Immunohistochemistry

At the time of necropsy, the circular defect area was cut in half with an Exakt bandsaw. The medial half of the repair tissue with surrounding native tissue was fixed in neutral-buffered

10% formalin for histology, and the lateral half was embedded in OCT and flash frozen for immunohistochemistry.

For histology, the fixed tissue was decalcified, embedded in paraffin, sectioned at 5 μm , and stained with either H&E or Safranin-O, fast green (SOFG) (ThermoScientific/Shandon VeriStain Gemini ES stainer) for proteoglycan visualization. Sections stained with H&E were evaluated blindly (DDF) using a modified O'Driscoll scoring system^{6,43} (Table 3) with a maximum cumulative histology score of 28 and a higher score indicating a repair more like native cartilage. Sections stained with SOFG were evaluated blindly (DDF) for intensity of staining on a scale of 0–3 (Table 3) and were included in the cumulative histology score.

For immunohistochemical analyses, frozen tissue was sectioned at 8 μm . Each section was incubated in 0.25 U/mL chondroitinase ABC (Sigma-Aldrich) for 15 min before incubation in primary antibody solution (Collagen I (1:10) #M-38-s and II (undiluted) # II-II6B3-s, Hybridoma Bank; Aggrecan (1:100, Alexis Biochemicals) #ALX-803-313; or rabbit IgG as control). Endogenous peroxidase was blocked using 0.3% H_2O_2 in methanol. Sections were incubated in goat anti-mouse HRP secondary antibody solution (1:500, Jackson ImmunoResearch, Westgrove, PA)), stained with Vector Nova RED (Vector Laboratories, Burlingame, CA) and counterstained with Fast Green. Controls gave no signal. Non-calcified tissues were evaluated blindly (DDF) for the percentage of repair tissue stained positive (0=no stain, 1=1–25%, 2=26–50%, 3=51–75%, 4=76–100%).

Radiographic Analysis

Radiographs and photographs were taken of bone segments from femoral sections. Radiographs were graded for presence of lysis, bony proliferation, osteophyte presence, and patellar luxation, and a total radiographic score was calculated by summing these scores (maximum score of 16). All grading was done on a 0–4 scale (0=none, 1=slight, 2=mild, 3=moderate, 4=severe)^{22,42}. Additionally, radiographs post-euthanasia were scored for healing of the defect (0=no healing, 1=slight healing, 2=mild bone filling, 3=lesion is visible but difficult to measure, 4=lesion not visible to measure), sclerosis around the defect, and other sclerosis (0–4, none-severe). Sclerosis is defined as the increase in density of bone seen radiographically and was subjectively scored by MFB in a blinded fashion.

Statistical Analyses

Scores were evaluated for inter- and intra-group differences using an ANOVA framework with PROC GLIMMIX (fits generalized linear mixed models) of SAS (Cary, NC)⁴⁴ with rabbit as a random variable. For all joint pathologic, histological, immunohistochemical, and radiographic analyses, intra-group differences were analyzed with treatment set as the main effect (one-way); differences among groups were analyzed using treatment and group as main effects (two-way). Untreated controls were therefore analyzed separately depending on what treatment the contralateral joint received in order to account for possible systemic effects⁴⁵. When main or interaction effects had p-values that were considered significant (p-value < 0.05) or a trend (0.05 < p-value < 0.10), individual comparisons were made using the least square means procedure²². P-values presented in the text include which main effect or interaction term they are referring to if quoted for comparisons among groups. All data are presented as mean \pm standard error of the mean (SEM). Non-parametric analyses were also performed when appropriate. The authors were able to reach similar conclusions based on either analysis. Because the authors feel many of the biologic outcome parameters represent more of a continuum rather than defined categories, the parametric analysis of the data is presented.

RESULTS

Radiographic Analyses

Radiographic analyses pre-treatment did not show any sclerosis in any of the rabbits. Treated defects post-treatment showed some slight osteophyte formation (0.3 (0.0, 0.6), treated; 0.1 (-0.2, 0.4), untreated; treatment $p=0.087$). There was no difference among groups (group $p=0.490$).

Gross Observation of Joints

Upon necropsy, joints and incision areas in all experimental groups appeared normal by gross examination (Fig 1), and no inflammation or infection was noted, indicating no adverse immune reaction to the treatments. Repair cartilage appeared to be moderately to normally attached to surrounding cartilage in all defects with no differences between treatments (treatment $p=0.299$) or groups (group $p=0.541$) (Table 4:XIII). Similarly, repair tissue ranged from normal to slightly-soft compared to surrounding tissue when assessed for attachment to the subchondral bone, with no differences between treatments (treatment $p=0.192$) or groups (group $p=0.970$) (Table 4:XIV). Rabbits receiving KLD+CF+BMSCs (group 3) demonstrated mild osteophyte formation, with an increased score compared to KLD-alone (group 1) (group $p=0.029$) (Table 4:VIII). Treated defects in group 3 also had better attachment to subchondral bone compared to untreated defects in group 3 ($p=0.030$) (Table 4:XIV). Overall, treated defects had an increased defect volume filled (91.4 (82.3, 100.4), treated vs. 78.2 (69.1, 87.3), untreated, treatment $p=0.032$) and the level of treated defects was higher than contralateral untreated defects (2.6 (2.3, 3.0), treated; 2.2 (1.8, 2.6), untreated; treatment $p=0.050$). Untreated defects also had more muscle wastage at the site of incision (assessed by circumferential measurement at the proximal aspect of the patella) (12.9 cm (12.5, 13.2), treated vs. 12.7 cm (12.3, 13.0), untreated; treatment $p=0.001$), with group 1 and 3 treated defects different from their respective contralateral controls (Table 4:III; interaction $p=0.032$). Treated defects were scored higher in grade of repair compared to contralateral untreated defects, equivalent to a score of good (3.0 (2.6, 3.5), treated vs. 2.5 (2.0, 2.9), untreated, on a scale of 0–4; treatment $p=0.061$).

Histologic Examinations

Synovial Membrane H&E: Evaluation of the synovial membrane by H&E staining showed some mild intimal hyperplasia and some mild to moderate vascularity and subintimal fibrosis, but there were no differences among any groups or treatments.

Articular Cartilage H&E: Assessment of the articular cartilage H&E staining showed that KLD (group 1) had a higher cumulative histology score compared to contralateral untreated controls when looking at that group alone (Table 5:XII, $p=0.034$). Overall, when comparing among groups, KLD and KLD+CF (groups 1 and 2) had higher cumulative scores than KLD+CF+BMSCs (group 3) (Table 5:XII, group $p=0.030$). Defects treated with KLD received the highest score for nature of predominant tissue in the defect (see Tables 3, 5:I), which was similar to fibrocartilage. The other groups and treatments ranged between 0 and 1, indicating presence of some fibrocartilage and some non-chondrocytic cells; however, none of the groups or treatments were significantly different (Table 5:I, group $p=0.749$, treatment $p=0.264$). Group 3 had significantly lower surface regularity with scores indicative of some fissuring of the surface (Tables 3,5:II, group $p=0.005$) and more degenerative change in cartilage surrounding the defect, showing mild to moderate hypocellularity compared to KLD and KLD+CF (Tables 3,5:VIII, group $p=0.015$). Group 2 had more reconstitution of subchondral bone than group 3 (group $p=0.030$), but all groups were still below normal subchondral bone levels (Tables 3,5: IX); treated defects trended higher than untreated defects (1.9 (1.5, 2.2) treated; 1.5 (1.1, 1.8) untreated; treatment $p=0.074$). Group 2 also

showed the highest score for bonding to adjacent cartilage (Table 5:V), but no groups or treatments were significantly different (treatment $p=0.161$, group $p=0.226$). Treated defects had increased cellularity (Table 3:VI) compared to contralateral untreated defects (treatment $p=0.031$) showing normal to slight hypocellularity in the treated defects repair tissue (1.8 (1.5, 2.0) treated; 1.6 (1.3, 1.8) untreated); group 3 trended higher than the other groups (2.0 (1.7, 2.3) group 3; 1.5 (1.1, 1.9) groups 1 and 2; group $p=0.081$).

Articular Cartilage SOFG—Defects treated with KLD-alone (group 1) had increased Safranin-O staining (scores of slight to moderate staining) than the contralateral untreated defects or treated defects in groups 2 and 3, which had only none to slight staining (Table 5:XI, interaction $p=0.011$). There was no overall effect of treatment or group on this measure (treatment $p=0.286$, group $p=0.604$). As shown in Fig 2, treatment with KLD-alone resulted in greater staining throughout the repair tissue.

Immunohistochemistry Evaluations

Looking at only group 1, defects treated with KLD showed increased collagen II immunostaining compared to contralateral untreated defects (Table 6:III, $p=0.028$); although aggrecan immunostaining for defects treated with KLD received a score of 2.7, it was not different from the contralateral untreated control (Table 6:I, $p=0.526$). This is in contrast to the difference observed in Safranin-O staining between defects treated with KLD and the contralateral untreated defects. In group 2, KLD+CF treatment elicited a tissue with higher aggrecan detected by immunostaining vs. the contralateral untreated control (Table 6:I, $p=0.041$). In addition, although defects treated with KLD+CF received the highest collagen II immunostaining score of all the groups, 3.4, this was not different from its contralateral untreated control (Table 6:III, $p=0.110$). Comparing all defects, treated defects had more collagen II (2.9 (2.2, 3.6) treated; 1.6 (0.9, 2.2) untreated; treatment $p=0.001$) and increased aggrecan (2.9 (2.3, 3.4) treated; 2.1 (1.6, 2.7) untreated; treatment $p=0.056$) compared to untreated defects; there were no differences among groups (group $p=0.293$). There were similar levels of collagen I immunostaining found in all the defects (treatment $p=0.471$, group $p=0.919$), consistent with the observation of mostly fibrocartilage seen in the gross scoring (Table 6:II). Overall, within the repair tissues, collagen II immunostaining was observed deeper in the sections and collagen I immunostaining was seen more in the superficial. Aggrecan immunostaining was noted to have a more generalized distribution, but more positive staining was seen deeper in the repair tissue.

DISCUSSION

Treatment of full-thickness articular cartilage defects with the self-assembling peptide KLD (group 1) markedly improved cartilage regeneration, as seen by significant increases in cumulative histology score, Safranin-O staining, and collagen II immunostaining, compared to critically-sized contralateral untreated defects. KLD has several advantages as a material due to its ability to be injected arthroscopically into a defect, assemble on contact with tissue, and promote cartilage regeneration without inducing an immune response. Adding TGF- β 1, dexamethasone, and IGF-1 to KLD (group 2) resulted in increased aggrecan immunostaining compared to its contralateral untreated defect, but in general did not result in any additional beneficial or deleterious effects compared to KLD alone (group 1). Motivated by *in vitro* results supporting BMSC chondrogenesis^{33,34,38}, we delivered these factors with allogeneic BMSCs in KLD *in vivo* (group 3). However, this treatment resulted in a poorer repair than with KLD or KLD+CF. This is similar to other reports of fibrous tissue formation after BMSC treatment^{23,24,26}, interpreted as a negative result.

In our rabbit model, the presence of a full-thickness defect allowed bone marrow to infiltrate the defect⁴⁶ and act as a cell source, similar to abrasion arthroplasty and subchondral bone microfracture surgical techniques. The positive healing response seen with KLD treatment (group 1) demonstrates that the scaffold supports cell migration and further chondrogenesis of these cells *in vivo*. The high porosity of this scaffold (~99.6% water content³¹) is in agreement with a recent *in vivo* study in rabbits by Ikeda et al.⁴⁷ demonstrating that scaffolds with >85% porosity promoted migration of bone marrow cells into polymer scaffolds and with an *in vitro* study by Wang et al.⁴⁸ demonstrating endothelial cell migration into several types of self-assembling hydrogels.

Regarding group 2, KLD+CF treatment, our results raise the issues of whether the CF dose was appropriate to improve endogenous cell response and whether cells migrating into the scaffold *in vivo* respond differently to these CFs than *in vitro* and thereby require different stimulation. The inclusion of CFs did not show increased chondrogenesis over KLD alone (group 1) as determined by cumulative histology score, Safranin-O, aggrecan, and type II collagen immunostaining. Similar to these results, Holland et al.¹³ reported that TGF- β 1 and IGF-1 delivered in gelatin microparticles within an acellular oligo(poly(ethylene glycol) fumarate) (OPF) scaffold resulted in repair no different than in empty defects, despite positive results *in vitro*. That study also delivered IGF-1 alone and found that this growth factor alone resulted in a significantly improved repair. In addition, other studies have looked at delivering IGF-1 alone *in vivo* and have reported similar positive results^{4,16}. While we did not test the effects of IGF-1 alone in this study, our results emphasize the need for further understanding of the combination of IGF-1 with other CF *in vivo* in order to take advantage of its characteristic anabolic properties.

The intra-articular use of TGF- β 1 remains controversial due to the pro-inflammatory response by the synovium seen at certain concentrations. Van der Kraan and van den Berg et al. have studied the interaction of TGF- β 1 with various joint tissues and have shown that while TGF- β 1 can stimulate proteoglycan production in cartilage, when it is exposed to synovial tissue, synovial fibrosis can occur; TGF- β 1-induced osteophyte formation is also common¹⁸. Mi et al.¹⁷ showed that injection of recombinant adenoviral vector for hTGF- β 1 into the knee joint space through the patellar tendon (resulting in ~8.75 ng TGF- β 1) dramatically increased joint inflammation, though this dose is more than 6-fold higher than our total dose of 1.4 ng. Accordingly, we did not observe these effects when TGF- β 1 was added to the peptide alone (group 2). In contrast, when TGF- β 1 was added in combination with BMSCs (group 3), osteophyte formation increased, suggesting an interaction of TGF- β 1 with these cells was responsible for the increased osteogenesis rather than the presence of TGF- β 1 alone in the joint (group 2). This finding is similar to results recently published by Guo et al.²⁷, in which 600 ng of TGF- β 1 per mL of hydrogel was used in combination with BMSCs in an OPF scaffold. Furthermore, we observed a detrimental increase in osteophyte formation and distortion of normal joint anatomy when, in the same rabbit, 1.4 ng TGF- β 1+BMSCs were placed in one joint and 0.7 ng TGF- β 1+BMSCs in the contralateral joint⁴⁹. The authors were surprised at this result given the total body dose of TGF- β 1 was only 1.5x what was used in group 2 or group 3 and the cell numbers 2-fold greater. While the amount of TGF- β 1 delivered in group 3 of our study was lower than that in the Mi¹⁷ study, and we attempted to deliver TGF- β 1 in a controlled fashion, it is still possible that this TGF- β 1 level was too high to beneficially induce chondrogenesis when combined with BMSCs, despite the inclusion of dexamethasone, which has been shown to enhance chondrogenesis compared to TGF- β 1 alone^{9,50}. A study by Fan et al. using only 0.8 ng of TGF- β 1 with BMSCs in a gelatin-chondroitin-hyaluronate tri-copolymer scaffold reported improved rabbit cartilage defect healing compared to treatment with BMSCs implanted in a scaffold without TGF- β 1. Taken together, these studies suggest that while the amount of TGF- β 1 we chose combined with BMSCs effectively induces chondrogenesis *in vitro*³⁸, additional

research is needed to determine a successful strategy for optimizing chondrogenesis of BMSCs *in vivo*, and interactions with synovial tissues must be considered.

Due to the often noted ability of cartilage defects in young/skeletally immature rabbits to heal well naturally⁴⁶, we used skeletally mature rabbits with average age of 11 months and critically-sized defects in order to test the ability of treatment to improve adult animal healing. Although full-thickness defects were used, defects only entered the subchondral/trabecular bone, resulting in contralateral untreated defects that do not heal spontaneously by 12 weeks. These results are similar to other studies using similar-aged rabbits and defect sizes. A limitation of our model is the lack of enough tissue to perform direct biochemical assessment in addition to histological and immunohistochemical measurements in this study. However, the purpose of the present study was to perform an initial trial prior to a larger animal study where such additional measures will be utilized, since ample tissue will be available.

In summary, the self-assembling peptide hydrogel KLD offers a new material suitable for further testing in a clinically relevant defect in a large animal. We demonstrated improved filling of osteochondral defects and improved cartilage repair, as seen by cumulative histology score, Safranin-O staining, and type II collagen immunostaining. In this small animal model, the full-thickness defect provided access to the marrow, similar in concept to abrasion arthroplasty or spongialization in large animal models (goat, sheep, horse, human), and suggests that combining KLD with these techniques may offer an improvement over current practice. Ongoing studies include the evaluation of KLD in a clinically relevant sized equine defect co-treated with microfracture and subjected to strenuous exercise, compared to defects treated with microfracture alone.

Acknowledgments

Supported in part by NIH Grants EB003805 and AR33236, NSF and NDSEG graduate fellowships (REM) and an Arthritis Foundation Postdoctoral Fellowship (EJV).

ROLE OF THE FUNDING SOURCE: NIH-NIBIB Grant EB003805; NDSEG and NSF graduate fellowships (RM); Arthritis Foundation Postdoctoral Fellowship (EJV).

References

1. Getgood A, Brooks R, Fortier L, Rushton N. Articular cartilage tissue engineering. *J Bone Joint Surg Br.* 2009; 91-B:565–576. [PubMed: 19407287]
2. Hoemann C, Sun J, McKee M, Chevrier A, Rossomacha E, Rivard G-E, et al. Chitosan-glycerol phosphate/blood implants elicit hyaline cartilage repair integrated with porous subchondral bone in microdrilled rabbit defects. *Osteoarthritis and Cartilage.* 2007; 15:78–89. [PubMed: 16895758]
3. Wang D-A, Varghese S, Sharma B, Strehin I, Fermanian S, Gorham J, et al. Multifunctional chondroitin sulphate for cartilage tissue-biomaterial integration. *Nat Mater.* 2007; 6:385–392. [PubMed: 17435762]
4. Nixon A, Fortier L, Williams J, Mohammed H. Enhanced repair of extensive articular defects by insulin-like growth factor-I-laden fibrin composites. *J Orthop Res.* 1999; 17:475–487. [PubMed: 10459752]
5. Wegener B, Schimpf F, Pietschmann M, Milz S, Berger-Loehr M, Bergschmidt P, et al. Matrix-guided cartilage regeneration in chondral defects. *Biotechnol Appl Biochem.* 2009; 53:63–70. [PubMed: 18795888]
6. Frisbie D, Bowman S, Colhoun H, DiCarlo E, Kawcak C, McIlwraith C. Evaluation of autologous chondrocyte transplantation via a collagen membrane in equine articular defects—results at 12 and 18 months. *Osteoarthritis and Cartilage.* 2008; 16:667–679. [PubMed: 18042409]

7. Janjanin S, Li W-J, Morgan MT, Shanti RM, Tuan RS. Mold-Shaped, Nanofiber Scaffold-Based Cartilage Engineering Using Human Mesenchymal Stem Cells and Bioreactor. *J Surg Res.* 2008; 149:47–56. [PubMed: 18316094]
8. Longobardi L, O'Rear L, Aakula S, Johnstone B, Shimer K, Chytil A, et al. Effect of IGF-I in the Chondrogenesis of Bone Marrow Mesenchymal Stem Cells in the Presence or Absence of TGF- β 1 Signaling. *J Bone Miner Res.* 2006; 21:626–636. [PubMed: 16598383]
9. Johnstone B, Hering TM, Caplan AI, Goldberg VM, Yoo JU. In Vitro Chondrogenesis of Bone Marrow-Derived Mesenchymal Progenitor Cells. *Experimental Cell Research.* 1998; 238:265–272. [PubMed: 9457080]
10. Indrawattana N, Chen G, Tadokoro M, Shann LH, Ohgushi H, Tateishi T, et al. Growth factor combination for chondrogenic induction from human mesenchymal stem cell. *Biochem Biophys Res Commun.* 2004; 320:914–919. [PubMed: 15240135]
11. Worster AA, Brower-Toland BD, Fortier LA, Bent SJ, Williams J, Nixon AJ. Chondrocytic differentiation of mesenchymal stem cells sequentially exposed to transforming growth factor- β 1 in monolayer and insulin-like growth factor-I in a three-dimensional matrix. *J Orthop Res.* 2001; 19:738–749. [PubMed: 11518286]
12. Jaklenc A, Hinckfuss A, Bilgen B, Ciombor DM, Aaron R, Mathiowitz E. Sequential release of bioactive IGF-I and TGF- β 1 from PLGA microsphere-based scaffolds. *Biomaterials.* 2008; 29:1518–1525. [PubMed: 18166223]
13. Holland TA, Bodde EWH, Cuijpers VMJI, Baggett LS, Tabata Y, Mikos AG, et al. Degradable hydrogel scaffolds for in vivo delivery of single and dual growth factors in cartilage repair. *Osteoarthritis Cartilage.* 2007; 15:187–197. [PubMed: 16965923]
14. Elisseeff J, McIntosh W, Fu K, Blunk T, Langer R. Controlled-release of IGF-1 and TGF- β 1 in a photopolymerizing hydrogel for cartilage tissue engineering. *J Orthop Res.* 2001; 19:1098–1104. [PubMed: 11781011]
15. Park K-H, Park W, Na K. Synthetic matrix containing glucocorticoid and growth factor for chondrogenic differentiation of stem cells. *J Biosci Bioeng.* 2009; 108:168–173. [PubMed: 19619866]
16. Schmidt M, Chen E, Lynch S. A review of the effects of insulin-like growth factor and platelet-derived growth factor on in vivo cartilage healing and repair. *Osteoarthritis Cartilage.* 2006; 14:403–412. [PubMed: 16413799]
17. Mi Z, Ghivizzani S, Lechman E, Glorioso J, Evans C, Robbins P. Adverse effects of adenovirus-mediated gene transfer of human TGF- β 1 into rabbit knees. *Arthritis Res Ther.* 2003; 5:R132–R139. [PubMed: 12723985]
18. Davidson ENB, van der Kraan P, van den Berg W. TGF- β and osteoarthritis. *Osteoarthritis Cartilage.* 2007; 15:597–604. [PubMed: 17391995]
19. Hunziker E. Growth-factor-induced healing of partial-thickness defects in adult articular cartilage. *Osteoarthritis Cartilage.* 2001; 9:22–32. [PubMed: 11178944]
20. Hwang NSP, Elisseeff JP. Application of Stem Cells for Articular Cartilage Regeneration. *J Knee Surg.* 2009; 22:60–71. [PubMed: 19216354]
21. Noth U, Steinert AF, Tuan RS. Technology Insight: adult mesenchymal stem cells for osteoarthritis therapy. *Nat Rev Rheumatol.* 2008; 4:371–380.
22. Frisbie D, Kisiday J, Kawcak C, Wery N, McIlwraith C. Evaluation of adipose-derived stromal vascular fraction or bone marrow-derived mesenchymal stem cells for treatment of osteoarthritis. *J Orthop Res.* 2009 in press.
23. Murphy J, Fink D, Hunziker E, Barry F. Stem cell therapy in a caprine model of osteoarthritis. *Arthritis Rheum.* 2003; 48:3464–3474. [PubMed: 14673997]
24. Wakitani S, Mitsuoka T, Nakamura N, Toritsuka Y, Nakamura Y, Horibe S. Autologous bone marrow stromal cell transplantation for repair of full-thickness articular cartilage defects in human patellae: two case reports. *Cell Transplant.* 2004; 13:595–600. [PubMed: 15565871]
25. Li W, Chiang H, Kuo T, Lee H, Jiang C, Tuan R. Evaluation of articular cartilage repair using biodegradable nanofibrous scaffolds in a swine model. *J Tissue Eng Regen Med.* 2009; 3:1–10. [PubMed: 19004029]

26. Wilke M, Nydam D, Nixon A. Enhanced early chondrogenesis in articular defects following arthroscopic mesenchymal stem cell implantation in an equine model. *J Orthop Res.* 2007; 25:913–925. [PubMed: 17405160]
27. Guo X, Park H, Young S, Kretlow J, van den Beucken J, Baggett L, et al. Repair of osteochondral defects with biodegradable hydrogel composites encapsulating marrow mesenchymal stem cells in a rabbit model. *Acta Biomaterialia.* 2010; 6:39–47. [PubMed: 19660580]
28. Diao H, Wang J, Shen C, Xia S, Guo T, Dong L, et al. Improved cartilage regeneration utilizing mesenchymal stem cells in TGF- β 1 gene-activated scaffolds. *Tissue Eng Part A.* 2009; 15:2687–2698. [PubMed: 19216641]
29. Fan H, Hu Y, Qin L, Li X, Wu H, Lv R. Porous gelatin-chondroitin-hyaluronate tri-copolymer scaffold containing microspheres loaded with TGF- β 1 induces differentiation of mesenchymal stem cells in vivo for enhancing cartilage repair. *J Biomed Mater Res A.* 2006; 77:785–794. [PubMed: 16575912]
30. Guo C-A, Liu X-G, Huo J-Z, Jiang C, Wen X-J, Chen Z-R. Novel gene-modified-tissue engineering of cartilage using stable transforming growth factor- β 1-transfected mesenchymal stem cells grown on chitosan scaffolds. *J Biosci Bioeng.* 2007; 103:547–556. [PubMed: 17630127]
31. Kisiday J, Jin M, Kurz B, Hung H, Semino C, Zhang S, et al. Self-assembling peptide hydrogel fosters chondrocyte extracellular matrix production and cell division: Implications for cartilage tissue repair. *Proc Natl Acad Sci USA.* 2002; 99:9996–10001. [PubMed: 12119393]
32. Erickson IE, Huang AH, Chung C, Li RT, Burdick JA, Mauck RL. Differential maturation and structure-function relationships in mesenchymal stem cell- and chondrocyte-seeded hydrogels. *Tissue Eng Part A.* 2009; 15:1041–52. [PubMed: 19119920]
33. Kisiday J, Kopesky P, Evans C, Grodzinsky AJ, McIlwraith C, Frisbie D. Evaluation of adult equine bone marrow- and adipose-derived progenitor cell chondrogenesis in hydrogel cultures. *J Orthop Res.* 2008; 26:322–331. [PubMed: 17960654]
34. Kopesky P, Vanderploeg E, Sandy J, Kurz B, Grodzinsky AJ. Self-assembling peptide hydrogels modulate in vitro chondrogenesis of bovine bone marrow stromal cells. *Tissue Eng Part A.* 2010; 16:465–477. [PubMed: 19705959]
35. Zhang S, Holmes T, Lockshin C, Rich A. Spontaneous Assembly of a Self-Complementary Oligopeptide to Form a Stable Macroscopic Membrane. *Proc Natl Acad Sci USA.* 1993; 90:3334–3338. [PubMed: 7682699]
36. Sieminski AL, Semino CE, Gong H, Kamm RD. Primary sequence of ionic self-assembling peptide gels affects endothelial cell adhesion and capillary morphogenesis. *J Biomed Mater Res A.* 2008; 87:494–504. [PubMed: 18186067]
37. Davis ME, Hsieh PCH, Takahashi T, Song Q, Zhang S, Kamm RD, et al. Local myocardial insulin-like growth factor 1 (IGF-1) delivery with biotinylated peptide nanofibers improves cell therapy for myocardial infarction. *Proc Natl Acad Sci USA.* 2006; 103:8155–8160. [PubMed: 16698918]
38. Kopesky P, Vanderploeg E, Kisiday J, Frisbie D, Sandy J, Grodzinsky A. Controlled delivery of TGF- β 1 by self-assembling peptide hydrogels induces chondrogenesis of bone marrow stromal cells and modulates Smad2/3 signaling. *Tissue Eng Part A.* 2010 In Press.
39. Florine, E.; Vanderploeg, E.; Kopesky, P.; Miller, R.; Grodzinsky, AJ. 56th Trans Orthop Res Soc. New Orleans: 2010. Dexamethasone Suppresses Aggrecan Catabolism in BMSC-seeded Peptide Hydrogels. (Abstract)
40. Wei X, Messner K. Age- and injury-dependent concentrations of transforming growth factor- β 1 and proteoglycan fragments in rabbit knee joint fluid. *Osteoarthritis Cartilage.* 1998; 6:10–18. [PubMed: 9616434]
41. Fortier LA, Mohammed HO, Lust G, Nixon AJ. Insulin-like growth factor-I enhances cell-based repair of articular cartilage. *J Bone Joint Surg Br.* 2002; 84-B:276–288. [PubMed: 11922373]
42. Frisbie D, Ghivizzani S, Robbins PD, Evans C, McIlwraith C. Treatment of experimental equine osteoarthritis by in vivo delivery of the equine interleukin-1 receptor antagonist gene. *Gene Ther.* 2002; 9:12–20. [PubMed: 11850718]

43. Rutgers M, van Pelt M, Dhert W, Creemers L, Saris D. Evaluation of histological scoring systems for tissue-engineered, repaired, and osteoarthritic cartilage. *Osteoarthritis Cartilage*. 2010; 18:12–23. [PubMed: 19747584]
44. The GLIMMIX Procedure. SAS Institute Inc; Cary, NC: 2006. p. 943
45. Homandberg G, Kang Y, Zhang J, Cole A, Williams J. A single injection of fibronectin fragments into rabbit knee joints enhances catabolism in the articular cartilage followed by reparative responses but also induces systemic effects in the non-injected knee joints. *Osteoarthritis Cartilage*. 2001; 9:673–683. [PubMed: 11795986]
46. Shapiro F, Koide S, Glimcher M. Cell origin and differentiation in the repair of full-thickness defects of articular cartilage. *J Bone Joint Surg Am*. 1993; 75:532–553. [PubMed: 8478382]
47. Ikeda R, Fujioka H, Nagura I, Kokubu T, Toyokawa N, Inui A, et al. The effect of porosity and mechanical property of a synthetic polymer scaffold on repair of osteochondral defects. *Int Orthop*. 2009; 33:821–828. [PubMed: 18415099]
48. Wang X, Horii A, Zhang S. Designer functionalized self-assembling peptide nanofiber scaffolds for growth, migration, and tubulogenesis of human umbilical vein endothelial cells. *Soft Matter*. 2008; 4:2388–2395.
49. Miller, R.; Grodzinsky, AJ.; Vanderploeg, E.; Lee, C.; Ferris, DJ.; Barrett, MF., et al. 56th Trans Orthop Res Soc. New Orleans: 2010. Repair of Full-Thickness Articular Cartilage Defect Using Self-Assembling Peptide, Growth Factors, and BMSCs. (Abstract)
50. Mouw JK, Connelly JT, Wilson CG, Michael KE, Levenston ME. Dynamic Compression Regulates the Expression and Synthesis of Chondrocyte-Specific Matrix Molecules in Bone Marrow Stromal Cells. *Stem Cells*. 2007; 25:655–663. [PubMed: 17124008]

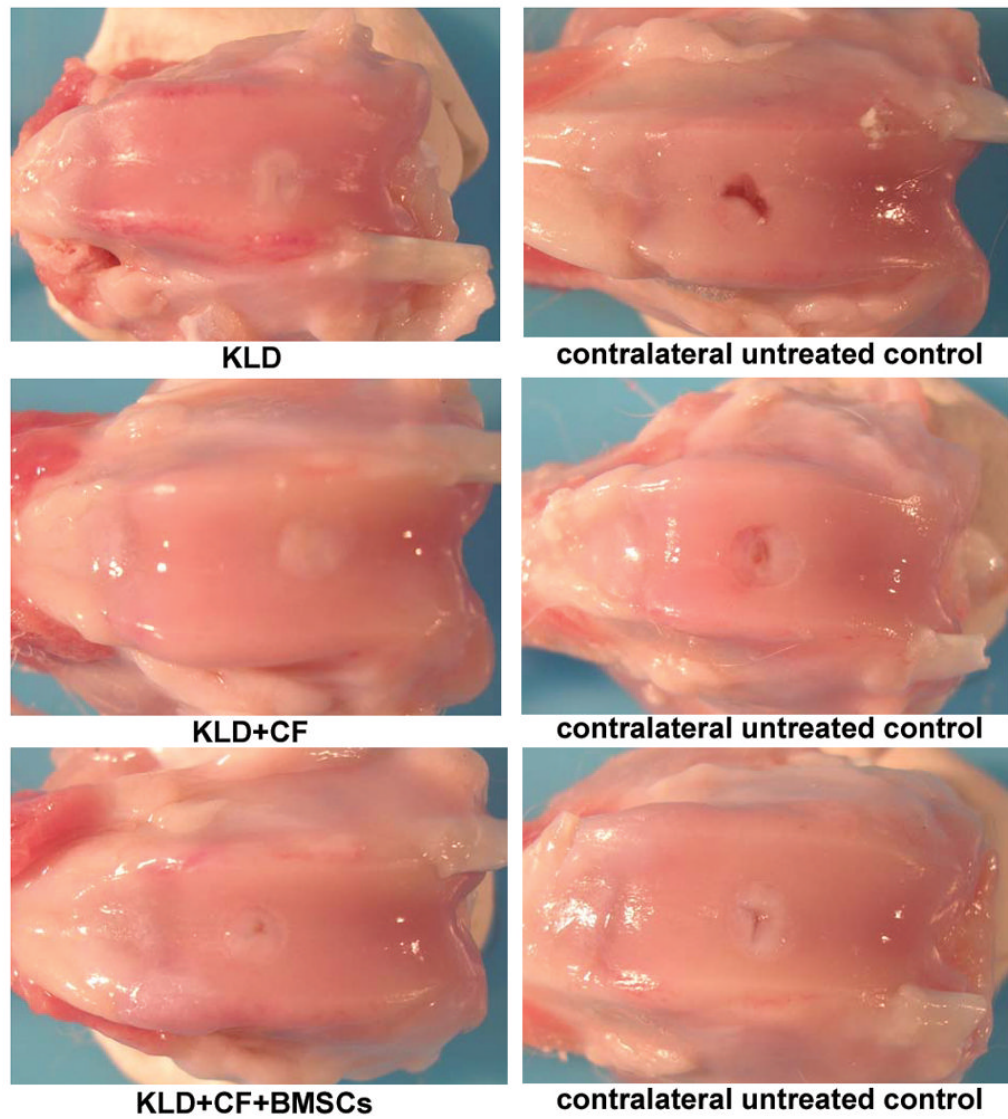


Fig 1. Gross necropsy photographs of treated and untreated joints in KLD, KLD+CF, and KLD+CF+BMSCs.

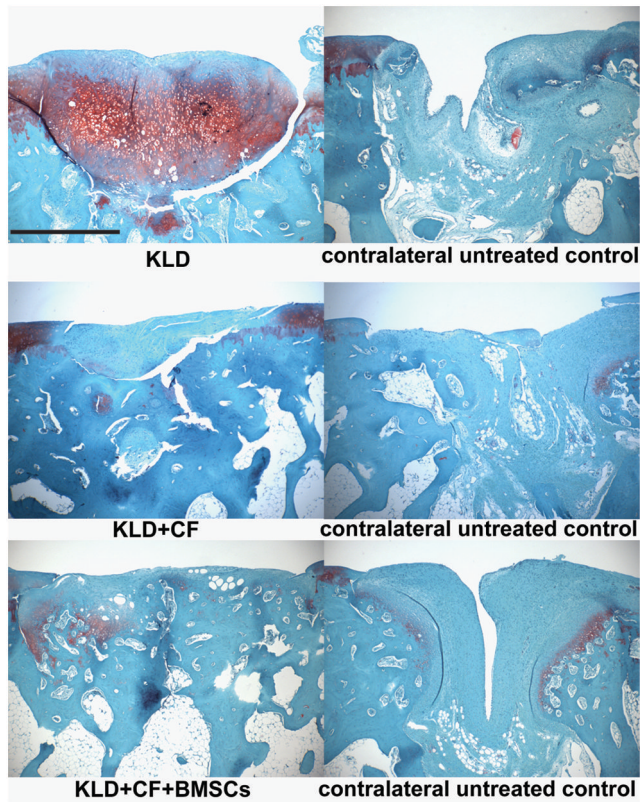


Fig 2. Safranin-O staining. Images showing histological evaluation of representative treatment groups and representative contralateral control knees. Treatment and contralateral pictures were representative of the mean scores and were taken from different animals for KLD and KLD+CF+BMSCs, and from the same animal for KLD+CF. Scale bar = 1 mm.

Table 1

Treatment groups with amounts delivered per animal.

Group	n	KLD (µg)	bKLD (µg)	TGF-β1 (ng)	bIGF (ng)	Streptavidin (ng)	Dex (ng)	BMSCs (×10 ³)
1 (KLD)	6	48	0.48	0	0	0	0	0
2 (KLD+CF)	6	48	0.48	1.4	4.1	30.7	0.6	0
3 (KLD+CF+BMSCs)	7	48	0.48	1.4	4.1	30.7	0.6	150

Table 2

Gross Observations Scoring System.

Feature	Score
I. Joint Observation	
Normal appearance	0
Slight inflammation	1
Moderate inflammation	2
Severe inflammation	3
II. Incision Appearance	
Normal appearance	0
Slight inflammation	1
Moderate inflammation	2
Severe inflammation	3
Slight dehiscence (incision basically intact)	4
Marked dehiscence (requires intervention)	5
Active infection	6
Healing infections	7
III. Muscle wastage at the time of necropsy in treated vs untreated limbs	
Circumferential measurement at the proximal aspect of the patella	(cm)
IV. Angle of Stifle: Change in normal angle (if any)	
None, within normal limits	0
Abnormal	1
V. Inflammation/Swelling	
None, within normal limits	0
Abnormal	1
VI. Trauma/Damage	
None, within normal limits	0
Abnormal	1
VII. Infection/Discharge	
None, within normal limits	0
Abnormal	1
VIII. Presence of Osteophytes and other Osteoarthritic Changes	
None, within normal limits	0
Abnormal	1
IX. Articular Surface Integrity, Contour, and Congruity	
Normal	0
Abnormal	1
X. Presence of Loose Bodies in Synovial Fluid	
None, within normal limits	0
Abnormal	1
XI. Injury to Apposing Articular Surface	
None, within normal limits	0

Feature	Score
Abnormal	1
XII. Synovial Membrane Appearance	
Normal	0
Slight	1
Mild	2
Moderate	3
Severe	4
XIII. Cartilage Attachment	
This category describes on average the defect repair tissue attachment with the surrounding normal cartilage. Possible responses were:	
Normal Attachment	0
Moderate Attachment	1
Mild Attachment	2
Slight Attachment	3
No Attachment	4
XIV. Bone Attachment	
This category describes the firmness of the repair tissue attachment to the bone at the base of the defect. Possible responses were:	
Similar to Surrounding Cartilage	0
Slightly Soft-vs-Surrounding Cartilage	1
Mildly Soft-vs-Surrounding Cartilage	2
Moderately Soft-vs-Surrounding Cartilage	3
Marked Softening-vs-Surrounding Cartilage	4
XV. Firmness	
This category describes on average the firmness of the repair tissue to normal surrounding articular cartilage. Possible responses were:	
Similar Compared to Surrounding Cartilage	0
Slightly Soft Compared to Surrounding Cartilage	1
Mildly Soft Compared to Surrounding Cartilage	2
Moderately Soft Compared to Surrounding Cartilage	3
Marked Softening Compared to Surrounding Cartilage	4
XVI. Blood	
This category describes the presence or absence of hemorrhage associated with the defect area or its periphery. Possible responses were:	
Fresh Blood, Active Hemorrhage at Time of Surgery	1
Old Blood, No Active Hemorrhage at Time of Surgery	2
No Blood Visualized at Time of Surgery	3
XVII. Shape	
This category describes the margin of the defect as it relates to the original geometry at time 0 (creation). Possible responses were:	
No Apparent in Damage Tissue Beyond Defect	0
Degeneration in Tissue Beyond Defect	1
XVIII. Grade (Overall quality of repair)	
This category describes the overall subjective evaluation of the repair tissue by the evaluator.	
Criteria used to determine the grade were:	
(1) Attachment of repair tissue to the surrounding normal articular cartilage	

Feature	Score
(2) Level (height) and undulation of the repair tissue surface as compared to the surrounding normal articular cartilage	
(3) Color of the repair tissue, where white homogenous tissue without a fibrous like appearance is used as the “gold standard.”	
Tissue Not Present to Grade	0
Poor	1
Fair	2
Good	3
Excellent	4
XIX. Level	
This category describes the level of repair tissue filling in association with the surrounding normal articular cartilage.	
Possible responses in relation to the surrounding normal articular cartilage were:	
Mildly Recessed	1
Slightly Recessed	2
Leveled	3
Slightly Elevated	4
Mildly Elevated	5
Moderately Elevated	6
XX. Color	
This category describes the color of the repair tissue. When repair tissue is characterized by two colors, the predominate color is indicated first. Possible responses were:	
Red	1
White/Red	2
Yellow	3
Yellow/White	4
White/Yellow	5
White	6
XXI. Surface	
This category describes the relative undulation of the repair tissue surface. Possible responses were:	
Non-Undulating	1
Slightly Undulating	2
Mildly Undulating	3
Moderately Undulating	4
XXII. Area	
Percent of Surface Area Filled in Defect	(0–100%)
XXIII. Volume	
Percent of Volume Filled in Defect	(0–100%)

Table 3

Modified O'Driscoll Histological Scoring System.

Feature	Score
I. Nature of the Repair Tissue	
Some Fibrocartilage, mostly nonchondrocytic cells	0
Mostly Fibrocartilage	1
Mixed Hyaline and Fibrocartilage	2
Mostly Hyaline Cartilage	3
Hyaline Cartilage	4
II. Surface Regularity	
Severe Disruption, Including Fibrillation	0
Fissures	1
Superficial Horizontal Lamination	2
Smooth and Intact	3
III. Structural Integrity (morphologic zone reconstitution)	
Severe Disintegration	0
Slight Disruption, Including Cysts	1
Normal	2
IV. Thickness	
0% – 50% of Normal Cartilage	0
50% – 100% of Normal Cartilage	1
100% of Normal Adjacent Cartilage	2
V. Bonding to Adjacent Cartilage	
Not Bonded	0
Bonded at One End or Partially at Both Ends	1
Bonded at Both Ends of Graft	2
VI. Hypocellularity	
Moderate Hypocellularity	0
Slight Hypocellularity	1
Normal Cellularity	2
VII. Chondrocyte Clustering	
25% – 100% of the Cells	0
< 25% of the Cells	1
No Clusters	2
VIII. Freedom from Degenerative Changes in Adjacent Cartilage	
Severe Hypocellularity, Poor or No Staining	0
Mild or Moderate Hypocellularity, Slight Staining	1
Normal Cellularity, Mild Clusters, Moderate Staining	2
Normal Cellularity, No Clusters, Normal Staining	3
IX. Reconstitution of Subchondral Bone	
No Subchondral Bone Reconstitution	0
Minimal Subchondral Bone Reconstitution	1

Feature	Score
Reduced Subchondral Bone Reconstitution	2
Normal	3
X. Inflammatory Response in Subchondral Bone Region	
Severe	0
Moderate	1
None/Mild	2
XI. Safranin-O Staining	
None	0
Slight	1
Moderate	2
Normal	3
XII. Cumulative Histology Score (sum of above scores)	0–28

Table 4

Gross Scores.

Gross Scores Feature	KLD		KLD+CF		KLD+CF+BMSCs		Two-way P-values
	treated n=6	untreated n=6	treated n=6	untreated n=6	treated n=7	untreated n=7	
I. Joint Observation	0 (0, 0)	0 (0, 0)	0 (0, 0)	0 (0, 0)	0 (0, 0)	0 (0, 0)	
II. Incision Appearance	0 (0, 0)	0 (0, 0)	0 (0, 0)	0 (0, 0)	0 (0, 0)	0 (0, 0)	
III. Muscle wastage at the time of necropsy in treated vs untreated limbs (circumference in cm)	12.8 (12.2, 13.4)	12.4 (11.8, 13.0), p=0.010	12.8 (12.2, 13.4)	12.7 (12.1, 13.3), p=0.530	13.0 (12.5, 13.6)	12.9 (12.4, 13.5), p=0.049	TXT: 0.001 Group: 0.553 TXT*Group: 0.032
IV. Angle of Stifle: Change in normal angle (if any)	0 (0, 0)	0 (0, 0)	0 (0, 0)	0 (0, 0)	0 (0, 0)	0 (0, 0)	
V. Inflammation/Swelling	0 (0, 0)	0 (0, 0)	0 (0, 0)	0 (0, 0)	0 (0, 0)	0 (0, 0)	
VI. Trauma/Damage	0 (0, 0)	0 (0, 0)	0 (0, 0)	0 (0, 0)	0 (0, 0)	0 (0, 0)	
VII. Infection/Discharge	0 (0, 0)	0 (0, 0)	0 (0, 0)	0 (0, 0)	0 (0, 0)	0 (0, 0)	
VIII. Osteophytes and other Osteoarthritic Changes	0.0 (-0.3, 0.3)	0.0 (-0.3, 0.3), p=1.000	0.2 (-0.2, 0.5)	0.2 (-0.2, 0.5), p=1.000	0.6 (0.3, 0.9)	0.6 (0.3, 0.9), p=1.000	TXT: 1.000 Group: 0.029 TXT*Group: 1.000
IX. Articular Surface Integrity, Contour, and Congruity	0 (0, 0)	0 (0, 0)	0 (0, 0)	0 (0, 0)	0 (0, 0)	0 (0, 0)	
X. Presence of Loose Bodies in Synovial Fluid	0 (0, 0)	0 (0, 0)	0 (0, 0)	0 (0, 0)	0 (0, 0)	0 (0, 0)	
XI. Injury to Opposing Articular Surface	0 (0, 0)	0 (0, 0)	0 (0, 0)	0 (0, 0)	0 (0, 0)	0 (0, 0)	
XII. Synovial Membrane	0.5 (0.0, 1.0)	0.3 (-0.1, 0.8), p=0.611	0.2 (-0.3, 0.6)	0.3 (-0.1, 0.8), p=0.562	0.1 (-0.3, 0.6)	0.3 (-0.1, 0.7), p=0.356	TXT: 0.750 Group: 0.685 TXT*Group: 0.605
XIII. Cartilage Attachment to surrounding cartilage	0.7 (0.0, 1.4)	1.0 (0.3, 1.7), p=0.530	0.5 (-0.2, 1.2)	0.3 (-0.4, 1.0), p=0.611	0.4 (-0.2, 1.1)	1.0 (0.3, 1.7), p=0.172	TXT: 0.299 Group: 0.541 TXT*Group: 0.423
XIV. Bone Attachment	0.3 (-0.3, 1.0)	0.7 (0.0, 1.3), p=0.363	0.7 (0.0, 1.3)	0.5 (-0.1, 1.1), p=0.695	0.3 (-0.3, 0.9)	0.9 (0.3, 1.5), p=0.030	TXT: 0.192 Group: 0.970 TXT*Group: 0.262
XV. Firmness	0.7 (-0.1, 1.5)	0.8 (0.0, 1.6), p=0.741	1.0 (0.2, 1.8)	0.5 (-0.3, 1.3), p=0.296	0.4 (-0.3, 1.2)	1.0 (0.3, 1.7), p=0.172	TXT: 0.750 Group: 0.995 TXT*Group: 0.222
XVI. Blood	3.0 (2.9, 3.1)	3.0 (2.9, 3.1), p=1.000	3.0 (2.9, 3.1)	3.0 (2.9, 3.1), p=1.000	3.0 (2.9, 3.1)	2.9 (2.7, 3.0), p=0.356	TXT: 0.384 Group: 0.449 TXT*Group: 0.449

Gross Scores Feature	KLD		KLD+CF		KLD+CF+BMSCs		Two-way P-values
	treated n=6	untreated n=6	treated n=6	untreated n=6	treated n=7	untreated n=7	
XVII. Shape	0 (0, 0)	0 (0, 0)	0 (0, 0)	0 (0, 0)	0 (0, 0)	0 (0, 0)	
XVIII. Grade (Overall quality of repair)	3.2 (2.3, 4.0)	2.2 (1.3, 3.0), p=0.076	2.7 (1.8, 3.5)	2.8 (2.0, 3.7), p=0.818	3.3 (2.5, 4.0)	2.4 (1.7, 3.2), p=0.017	TXT: 0.061 Group: 0.896 TXT*Group: 0.220
XIX. Level	2.7 (2.0, 3.3)	2.0 (1.3, 2.7), p=0.102	2.5 (1.8, 3.2)	2.3 (1.7, 3.0), p=0.695	2.7 (2.1, 3.3)	2.3 (1.7, 2.9), p=0.200	TXT: 0.050 Group: 0.897 TXT*Group: 0.613
XX. Color	5.8 (4.7, 6.9)	4.7 (3.6, 5.8), p=0.126	4.8 (3.7, 5.9)	4.8 (3.7, 5.9), p=1.000	5.9 (4.8, 6.9)	5.3 (4.3, 6.3), p=0.231	TXT: 0.182 Group: 0.363 TXT*Group: 0.547
XXI. Surface	1.8 (1.2, 2.5)	2.2 (1.5, 2.8), p=0.465	1.5 (0.8, 2.2)	2.0 (1.3, 2.7), p=0.296	1.7 (1.1, 2.3)	2.0 (1.4, 2.6), p=0.457	TXT: 0.127 Group: 0.753 TXT*Group: 0.925
XXII. Area	94.2 (80.2, 108.2)	90.0 (76.0, 104.0), p=0.383	95.7 (81.7, 109.7)	90.0 (76.0, 104.0), p=0.441	97.1 (84.2, 110.1)	82.9 (69.9, 95.8), p=0.276	TXT: 0.138 Group: 0.902 TXT*Group: 0.681
XXIII. Volume	91.7 (75.6, 107.8)	71.7 (55.6, 87.8), p=0.058	88.2 (72.1, 104.3)	80.8 (64.7, 96.9), p=0.477	94.3 (79.4, 109.2)	82.1 (67.2, 97.0), p=0.297	TXT: 0.032 Group: 0.706 TXT*Group: 0.667

One-way p-values for within group comparisons are listed in the untreated columns. Two-way p-values for differences among groups are in a separate column (TXT = treatment, Group = group, TXT*Group = interaction term). P-values are not shown when all the scores being compared are zero. Mean and confidence intervals calculated during two-way analysis are shown.

Table 5

Histological Scores.

Histology Scores Feature	KLD		KLD+CF		KLD+CF+BMSCs		Two-way P-values
	treated n=6	untreated n=6	treated n=6	untreated n=6	treated n=7	untreated n=7	
I. Nature of the Repair Tissue	1.0 (0.4, 1.6)	0.7 (0.1, 1.3), p=0.363	0.7 (0.1, 1.3)	0.7 (0.1, 1.3), p=1.000	0.9 (0.3, 1.4)	0.4 (-0.1, 1.0), p=0.134	TXT: 0.264 Group: 0.749 TXT*Group: 0.710
II. Surface Regularity	2.5 (1.8, 3.2)	2.2 (1.5, 2.9), p=0.175	2.0 (1.3, 2.7)	1.7 (1.0, 2.4), p=0.465	1.4 (0.8, 2.1)	0.9 (0.2, 1.5), p=0.298	TXT: 0.130 Group: 0.005 TXT*Group: 0.906
III. Structural Integrity	1.3 (0.9, 1.7)	1.0 (0.6, 1.4), p=0.175	1.2 (0.8, 1.6)	1.2 (0.8, 1.6), p=1.000	0.9 (0.5, 1.2)	0.7 (0.3, 1.1), p=0.563	TXT: 0.284 Group: 0.118 TXT*Group: 0.655
IV. Thickness	1.7 (1.1, 2.2)	1.2 (0.6, 1.7), p=0.237	1.5 (1.0, 2.0)	1.7 (1.1, 2.2), p=0.611	1.3 (0.8, 1.8)	1.3 (0.8, 1.8), p=1.000	TXT: 0.583 Group: 0.478 TXT*Group: 0.396
V. Bonding to Adjacent Cartilage	0.7 (0.1, 1.3)	1.0 (0.4, 1.6), p=0.363	1.3 (0.7, 1.9)	1.3 (0.7, 1.9), p=1.000	0.6 (0.0, 1.1)	1.0 (0.4, 1.6), p=0.200	TXT: 0.161 Group: 0.226 TXT*Group: 0.580
VI. Hypocellularity	1.7 (1.3, 2.1)	1.3 (0.9, 1.7), p=0.175	1.7 (1.3, 2.1)	1.3 (0.9, 1.7), p=0.175	2.0 (1.6, 2.4)	2.0 (1.6, 2.4), p=1.000	TXT: 0.031 Group: 0.081 TXT*Group: 0.259
VII. Chondrocyte Clustering	1.7 (1.3, 2.0)	1.8 (1.5, 2.2), p=0.363	1.7 (1.3, 2.0)	1.7 (1.3, 2.0), p=1.000	1.9 (1.5, 2.2)	2.0 (1.7, 2.3), p=0.356	TXT: 0.364 Group: 0.397 TXT*Group: 0.809
VIII. Freedom from Degenerative Changes in Adjacent Cartilage	1.7 (1.2, 2.2)	1.8 (1.3, 2.3), p=0.611	1.8 (1.3, 2.3)	2.2 (1.7, 2.7), p=0.363	1.3 (0.8, 1.8)	1.0 (0.5, 1.5), p=0.172	TXT: 0.658 Group: 0.015 TXT*Group: 0.270
IX. Reconstitution of Subchondral Bone	1.8 (1.2, 2.4)	1.5 (0.9, 2.1), p=0.363	2.2 (1.6, 2.8)	2.0 (1.4, 2.6), p=0.695	1.6 (1.0, 2.1)	0.9 (0.3, 1.4), p=0.074	TXT: 0.074 Group: 0.030 TXT*Group: 0.556
X. Inflammatory Response in Subchondral Bone Region	2.0 (1.9, 2.1)	1.8 (1.7, 2.0), p=0.363	2.0 (1.9, 2.1)	2.0 (1.9, 2.1), p=1.000	2.0 (1.9, 2.1)	2.0 (1.9, 2.1), p=1.000	TXT: 0.306 Group: 0.358 TXT*Group: 0.358
XI. Safranin-O Staining	1.2 (0.6, 1.7)	0.2 (-0.4, 0.7), p=0.012	0.3 (-0.2, 0.9)	0.5 (-0.0, 1.0), p=0.611	0.3 (-0.2, 0.8)	0.6 (0.1, 1.1), p=0.337	TXT: 0.286 Group: 0.604 TXT*Group: 0.011
XII. Cumulative Histology Score (sum of above scores)	17.2 (14.8, 19.5)	14.5 (12.2, 16.8), p=0.034	16.3 (14.0, 18.7)	16.2 (13.8, 18.5), p=0.915	14.0 (11.8, 16.2)	12.7 (10.5, 14.9), p=0.417	TXT: 0.140 Group: 0.030 TXT*Group: 0.541

One-way p-values for within group comparisons are listed in the untreated columns. Two-way p-values for differences among groups are in a separate column (TXT = treatment, Group = group, TXT*Group = interaction term). Mean and confidence intervals calculated during two-way analysis are shown.

Table 6

Immunohistochemical Scores.

IHC Scores Feature	KLD		KLD+CF		KLD+CF+BMSCs		Two-way p-values TXT: 0.056 Group: 0.384 TXT*Group: 0.857
	treated	untreated	treated	untreated	treated	untreated	
I. Aggrecan	2.7 (1.7, 3.6) n=6	2.2 (1.2, 3.1), p=0.526, n=6	3.3 (2.4, 4.3) n=6	2.3 (1.4, 3.3), p=0.041, n=6	2.6 (1.7, 3.5) n=7	1.9 (1.0, 2.7), p=0.253, n=7	TXT: 0.056 Group: 0.384 TXT*Group: 0.857
II. Collagen I	2.7 (1.5, 3.9) n=6	3.0 (1.8, 4.2), p=0.638, n=6	2.8 (1.5, 4.1) n=5	3.3 (2.1, 4.5), p=0.528, n=6	2.8 (1.6, 4.0) n=6	3.0 (1.8, 4.2), p=0.858, n=6	TXT: 0.471 Group: 0.919 TXT*Group: 0.950
III. Collagen II	3.2 (2.0, 4.3) n=6	1.3 (0.2, 2.5), p=0.028, n=6	3.3 (2.1, 4.5) n=5	2.2 (1.0, 3.3), p=0.110, n=6	2.2 (1.0, 3.3) n=6	1.2 (0.0, 2.3), p=0.144, n=6	TXT: 0.001 Group: 0.293 TXT*Group: 0.551

One-way p-values for within group comparisons are listed in the untreated columns. Two-way p-values for differences among groups are in a separate column (TXT = treatment, Group = group, TXT*Group = interaction term). Mean and confidence intervals calculated during two-way analysis are shown.